



## EXPERIMENTAL STUDY ON MASONRY WALLS USING AAC BLOCKS

K. Takashima<sup>(1)</sup>, S. Nakata<sup>(2)</sup>, R. Nakamura<sup>(3)</sup>, H. Iida<sup>(3)</sup>, T. Hanai<sup>(3)</sup>, A. Tasai<sup>(4)</sup>

<sup>(1)</sup> Asahi-kasei Homes Co., [takashima.kf@om.asahi-kasei.co.jp](mailto:takashima.kf@om.asahi-kasei.co.jp)

<sup>(2)</sup> Asahi-kasei Homes Co.

<sup>(3)</sup> Ebisu Building Laboratory Co.

<sup>(4)</sup> Yokohama National University

### ABSTRACT

An Autoclaved aerated concrete (AAC) masonry is an efficient structural system because its light weight resulted from its material characteristics by its own cellular structure reduces seismic inertia forces under earthquake excitations. Moreover, its light weight also improves workability at its construction site and thermal insulation quality for comfortable environments.

In this research, the masonry wall was constituted by two types of AAC blocks. One was reinforced with internal bar and the other was unreinforced. Both cases had grooves and vertical holes. Vertical reinforcements were cast in the holes while horizontal re-bars were cast in the groove. The grooves and holes were fully grouted in order to achieve a good bonding behavior between the bars and blocks.

Compression wallette tests and shear wallette tests were carried out and the mechanical properties of the masonry wall and the behavior of the wallettes were obtained. The confinement under the compressive force and the shear reinforcing effect of the internal reinforcement in the blocks under the shear force avoided the sharp post-peak drop and enhanced displacement capacity.

The in-plane behavior of bearing walls built with the AAC blocks was assessed by experimental tests. The integrated wall behavior was observed in the test results which revealed that the AAC masonry units were sufficiently bonded each other. The internal reinforcements improve those post-peak behavior and enhance displacement capacity as in the case of wallette tests. Moreover, stiffness of the 4.5m long wall was higher than that of the 1.5m long wall because a flexural deformation of the 4.5m long wall was obviously lower than that of the 1.5m long wall.

The basic consideration of the bearing wall test results referring to ordinary RC beam were carried out because the integrated behavior was observed. The bearing wall was considered as a cantilever beam that has an effective cross section according to Navier's hypothesis. The AAC and grout were considered as a homogeneous material which has an effective compressive strength and stiffness obtained from wallette tests. For the sake of easiness, only the vertical reinforcements which were cast in the both ends of the walls were considered. The strength and deformation were calculated and then compared to the experimental results. The flexural cracking strength of the experimental result showed good agreement with the calculated values however the shear strength were lower than those calculated values. Furthermore, the flexural cracking deformation of the wall with reinforced blocks obtained from experimental result was predicted by those calculations. The yield strength and ultimate strengths obtained from experimental results were higher than those of calculation, therefore the calculation model needs further modification for improvement in its precision.

*Keywords: AAC block; internal bar; wallette; bearing wall; in-plane behavior*

### 1. INTRODUCTION

Masonry can be considered as the oldest structural system and still being used in today's buildings around the world. However unreinforced masonry buildings do not behave well under earthquake excitations. In addition, it is well-known that comfortable environment is caused by sufficient thermal insulation quality. Therefore, Autoclaved aerated concrete (AAC) masonry is efficient structural system rather than using sliced stones, clay bricks and concrete blocks because its light weight resulted from material characteristics by its own cellular structure reduces the seismic inertia forces under earthquake excitations and improves thermal insulation quality.



Moreover, its light weight improves also workability at its construction site and its non-combustible and fire-resisting characteristics has an advantage against fires commonly associated with earthquakes.

The seismic behavior of reinforced AAC masonry piers has been assessed by cyclic tests of bearing walls in [1]. It has been found that confined masonry with horizontal reinforcement provide a significant increment of the strength and displacement capacity. In case of walls reinforced with only horizontal reinforcement, the displacement capacity was enlarged to the same level of the confined walls. However, the usual structural system that every layer was mortared and R.C. columns were cast in the walls is time-consuming job.

Therefore, a masonry structural system that a masonry wall was grouted after blocks were built was considered referring to in [2]. It was expected that the masonry structure is integrated under lateral force because the blocks were bonded each other with the high mobility grout. In addition, it was expected that using AAC blocks reinforced with internal bars which usually used in AAC panels is more effective for seismic behavior than using unreinforced AAC blocks.

This paper provide the mechanical properties revealed by material tests and wallette tests and then that in-plane behavior of bearing walls with different masonry blocks was compared and evaluated. Furthermore, basic consideration was carried out with the bearing wall test results referring to ordinary RC beam.

## 2. MASONRY MATERIALS AND STRUCTURAL SYSTEM

Two types of AAC blocks are shown in Table 2.1 and the block configurations and structural system of bearing walls are shown in Fig. 2.1.

Masonry walls were constituted by two types of AAC blocks. One had nominal dimensions of 750 x 150 x 250mm (wide  $w_b$ , height  $h_b$  and thickness  $t_b$ ) and specific gravity in oven-dry of 3.7 kN/m<sup>3</sup> (AAC(37)). The other had nominal dimensions of 500 x 200 x 250mm and specific gravity in oven-dry of 4.2 kN/m<sup>3</sup> (AAC(42)). AAC(37) was reinforced with 3.2mm internal bars and AAC(42) was unreinforced. Both cases had grooves of wide 150mm and depth 15mm from the bottom and sides and 50mm diameter vertical holes at 250mm spacing. Vertical reinforcements of 20mm had screws at both ends and they were cast in the vertical holes of the blocks at 750mm spacing. The vertical bars were jointed to anchor bolts embedded in grade beams with high nuts. Horizontal re-bar of 10mm were cast in the bottom grooves of the blocks at 600mm spacing. The blocks were pasted with sealant and built. The grooves and vertical holes were fully grouted in order to achieve a good bonding behavior between the bars and blocks.

Mechanical properties of the materials presented in Table 2.2 show mean values obtained from test results.

Compression tests of the AAC referring to Japanese Industrial Standard: JIS A 5416-2007, compression tests of the grout referring to JSCE Standard Specifications for Concrete Structures: JSCE-G 521-2013 and tensile tests of the bars referring to JIS Z 2241-2011 were carried out. Test setups used were an amsler testing machine or an electromechanical universal testing machine. Maximum strength was obtained from maximum force per cross sectional area. Yield point was obtained from upper yield point of vertical and horizontal bars and 0.2% offset yield strength of internal bars. Young modulus was obtained from secant stiffness between the origin point and one-third point of the maximum stress in stress - strain curve. The strain was obtained from strain gauges on the test specimens. AAC(37) has more tobermorite content than general AAC including AAC(42). Therefore the strength and Young modulus of AAC(37) were about higher than AAC(42) though the specific gravity was lower.

Table 2.1 Types of AAC blocks

block type	internal bars	configuration ( $w_b \times h_b \times t_b$ )	specific gravity (oven-dty)
AAC(37)	exist	750 x 150 x 250mm	0.37 kN/m <sup>3</sup>
AAC(42)	non	500 x 200 x 250mm	0.42 kN/m <sup>3</sup>

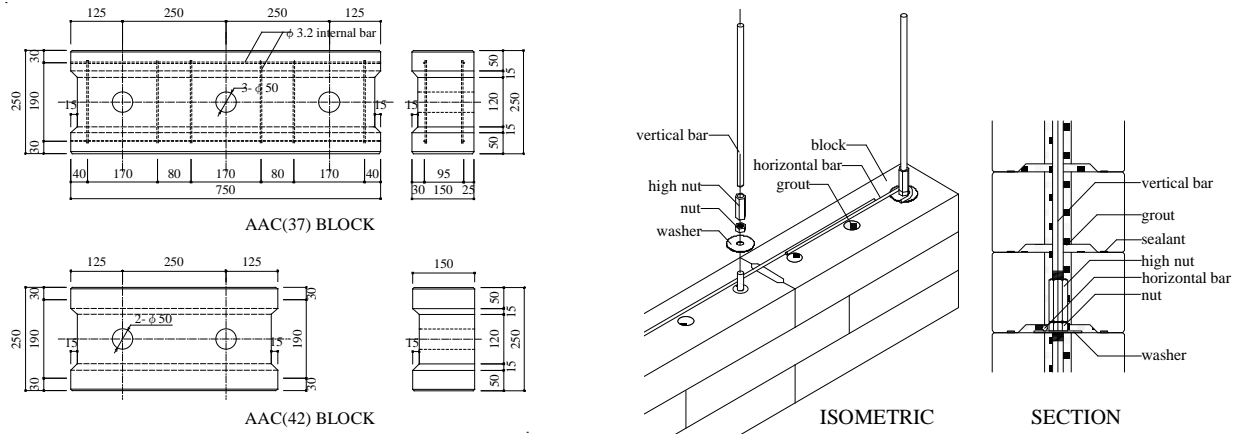


Fig. 2.1 Block configurations and Structural system

Table 2.2 Mechanical properties of materials

test	material	test specimen (mm)	number	yield point (N/mm <sup>2</sup> )	strength (N/mm <sup>2</sup> )	Young modulus (kN/mm <sup>2</sup> )
tensile	vertical bar	φ20 x 500	3	354	560	208
	horizontal bar	φ10 x 450	3	363	508	202
	internal bar	φ3.2 x 600	9	673	686	214
	AAC(37)	φ50 x 100	6	-	0.61	1.67
	AAC(42)		5	-	0.66	1.45
compression	AAC(37)	75 x 75 x 75	6	-	3.3	1.71
	AAC(42)	100 x 100 x 100	5	-	2.7	1.04
	grout	φ50 x 100	18	-	42.4	17.6

### 3. WALLETTE TEST

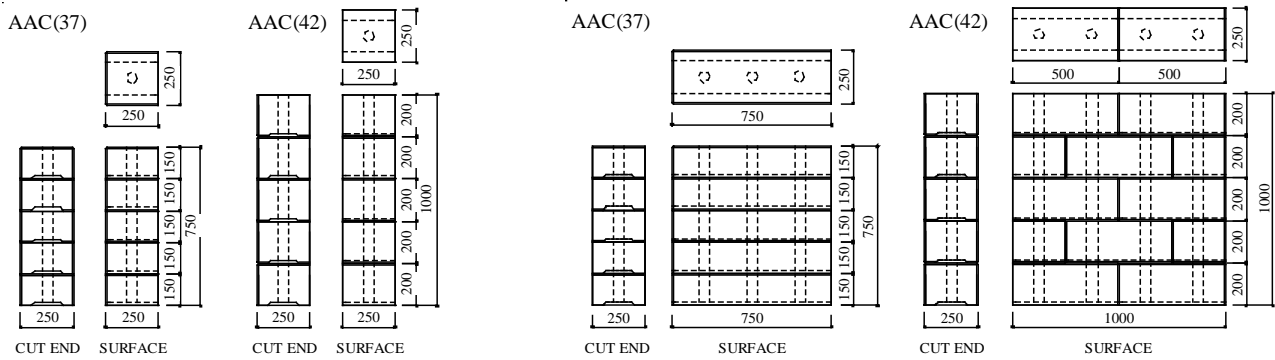
#### 3.1 TEST SPECIMENS AND TEST SETUP

Test schemes are shown in Table 3.1, Configurations of test specimens are shown in Fig. 3.1 and test setups are shown in Fig. 3.2.

Three specimens constituted by AAC(37) or AAC(42) were carried out each in case of compression tests and shear tests. Test setup used was an amsler testing machine. Force and axial deformations were measured in case of compression test and force and diagonal deformations were measured in the case of shear test.

Table 3.1 Test schemes

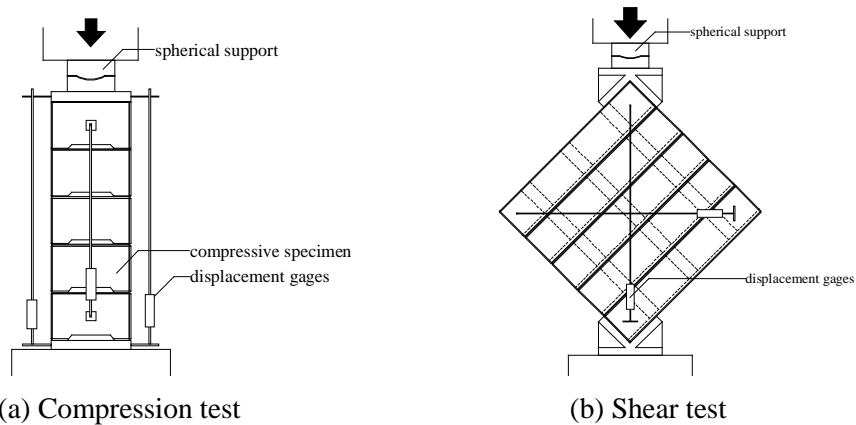
test	blocks	configurations (mm)	number
compression	AAC(37)	250 x 750 x 750	3
	AAC(42)	250 x 250 x 1000	3
shear	AAC(37)	750 x 750 x 250	3
	AAC(42)	1000 x 1000 x 250	3



(a) Compression test

(b) Shear test

Fig. 3.1 Test specimen



(a) Compression test

(b) Shear test

Fig. 3.2 Test setup

### 3.2 TEST RESULTS AND BEHAVIOR

#### 3.2.1 COMPRESSION TEST

Final cracking patterns and pictures of the specimens at the end of compression test are shown in Fig. 3.3.

The specimens used with AAC(37) developed vertical cracks immediately before maximum force followed by those cracks proceeded towards the axial direction in post-peak. The cracks of the cut ends were observed near internal bars and corners of the bottom grooves of the blocks. The specimens used with AAC(42) developed first vertical cracks in central part of surfaces of the blocks at half of the maximum force. Thereafter the cracks of the cut ends were observed near corners of the bottom grooves immediately before the maximum force and those cracks proceeded towards the axial direction in post-peak.

Representative compressive stress - strain curves are shown in Fig. 3.4.

It was found that the stress - strain curve shows a straight line right before the maximum force in specimens. The stress was obtained from the force per cross section area. As for the AAC(37) specimens, post-peak drop was observed in post-peak and the deformation proceeded while the force kept about 70% of the maximum force. Thereafter the strain achieved 1% in half of the maximum force. As for the AAC(42) specimens, sharp post-peak drop was observed in post-peak and the strain achieved 0.2% in half of the maximum force.

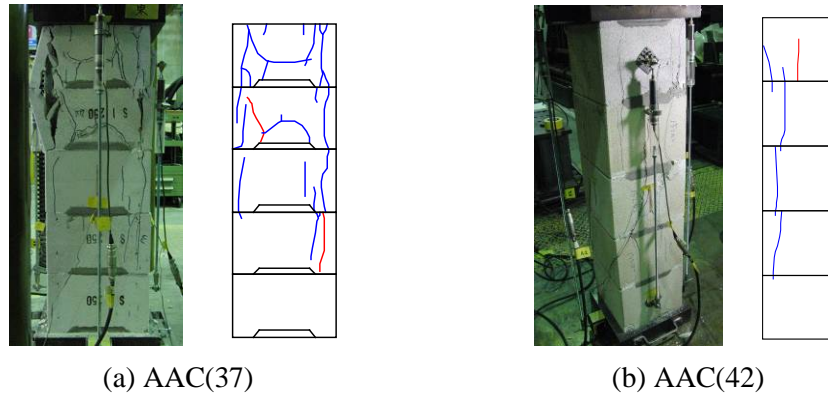


Fig. 3.3 Final cracking patterns and Pictures of the specimens at the end of compression test

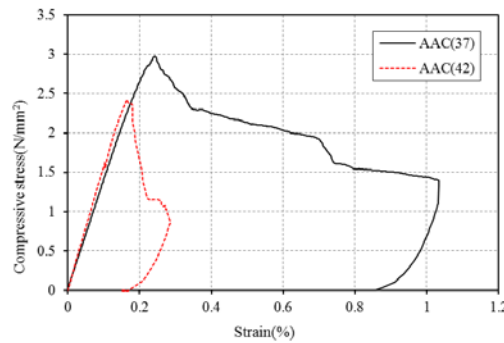


Fig. 3.4 Compression stress - Strain curve

Mean values of compression test results are shown in Table.3.2

The blocks were built after sealant was applied to the bottom of the blocks in order to prevent grout from leaking in joints of the walls. There was a slight space between each surfaces of the blocks and the groove and holes of the blocks were grouted. Therefore, it is considered that the stress in the walls is transferred in contact parts of the blocks and grout (effective cross section,  $A_e$ ). Accordingly, effective compressive strength and effective Young modulus was obtained from using  $A_e$  in addition to all cross section,  $A$ . The strain was obtained at the maximum force,  $P_{max}$  and 85% of the maximum force,  $0.85P_{max}$ . The strain of  $0.85 P_{max}$  was used in the fifth section for stress block coefficient in ultimate moment.

Table 3.2 Compression test results

block type	compressive strength (N/mm <sup>2</sup> )		Young modulus (N/mm <sup>2</sup> )		strain (%)	
	$A$	$A_e$	$A$	$A_e$	$P_{max}$	$0.85P_{max}$
AAC(37)	2.8	4.6	1211	2015	0.24	0.30
AAC(42)	2.4	3.9	1407	2346	0.18	0.19

### 3.2.2 SHEAR TEST

Final cracking patterns and pictures of the specimens at the end of shear tests are shown in Fig. 3.5.

Shear cracks developed when shear strain achieved about 0.1% in all specimens. The AAC(37) specimens developed new shear cracks and a drift at one of bed joints between each blocks was observed in post-peak. As for AAC(42), the shear cracks proceeded and widened extremely. It is considered that the internal bars avoid progress and widening of the shear cracks.

Representative shear stress - shear strain curves are shown in Fig. 3.6. The shear-stress,  $\tau$  was given by Eq. 3.1 and the shear-strain,  $\gamma$  was given by Eq. 3.2 and shown in Fig 3.6.

The shear stress - shear strain curve showed a straight line right before maximum force. As for AAC(37), post-peak drop was observed in post-peak and the shear strain achieved about 2% in half of maximum force. As for AAC(42), the sharp post-peak drop was observed and the shear strain achieved 0.5 % in half of maximum force. It is considered that shear reinforcing effect of the internal bars avoid sharp post-peak drop and enhance displacement capacity.

The mean value of shear test results is shown in Table.3.3

As with compression test, the shear strength and shear modulus was obtained from using both  $A_e$  and  $A_c$ .

$$\tau = P / t_s l_s \sin\alpha \tag{3.1}$$

$$\gamma = (\delta_1 \cos\alpha + \delta_2 \sin\alpha) / (x_s - \delta_2 \sin\alpha / 2 - \delta_2 \sin\alpha / 2) \tag{3.2}$$

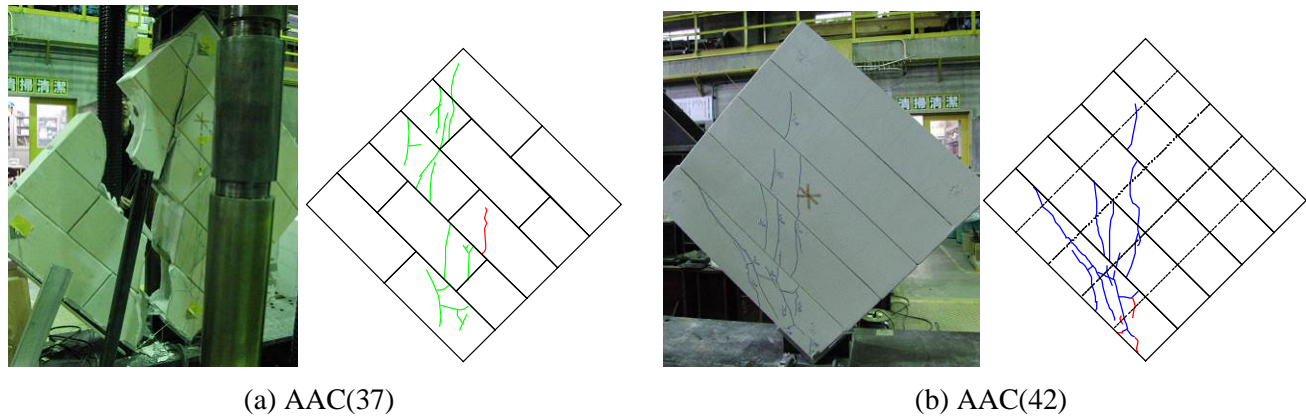


Fig. 3.5 Final cracking patterns and Pictures of the specimens at the end of shear test

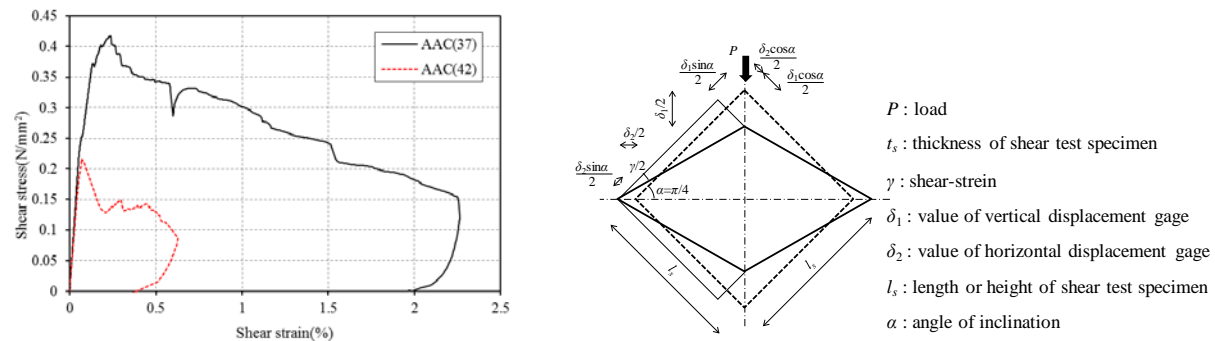


Fig. 3.6 Shear stress - Shear strain curve

Table 3.3 Shear test results

block type	shear strength (N/mm <sup>2</sup> )		shear modulus (N/mm <sup>2</sup> )		strain (%)
	A	A <sub>e</sub>	A	A <sub>e</sub>	P <sub>max</sub>
AAC(37)	0.41	0.69	303	504	0.23
AAC(42)	0.20	0.33	265	441	0.08

## 4. IN-PLANE TEST OF BEARING WALL

### 4.1 TEST SPECIMENS AND TEST SETUP

In-plane tests of bearing walls were carried out on full scale masonry walls built with the two types of AAC blocks. Test schemes are shown in Table 4.1, Test setup is shown in Fig. 4.1 and configurations of test specimens are shown in Fig. 4.2, target story drift levels are shown in Table 4.2.

Two walls with a length *l* of 1.5m and 4.5m were built with AAC(37) blocks and the other with a length *l* of 1.5m was built with AAC(42) blocks. A reinforced concrete top beam was built in each wall in order to distribute better the applied lateral force and vertical load as sustained load. The vertical load resulted in a load ratio (ratio of average vertical stress to compression strength obtained from the wallette compression tests) of about 0.01. The vertical holes which the vertical reinforcements were cast in were grouted and the others were not grouted with the aim of electrical wiring in the holes.

Test setup used was a cantilever system which was fixed at the base and free at the top. Horizontal force was applied by a displacement-controlled horizontal hydraulic actuator, performing cyclic force for each target story drift level. The story drift of the test specimen was obtained from the remainder between lateral displacement at the top and bottom of specimen divided by height between two displacement gages.

Table 4.1 Test schemes

block type	internal bars	length (m)	height (m)	thickness (m)	vertical reinforcement	horizontal re-bar
AAC(37)	exist	1.5	3	0.25	φ20	φ10
AAC(37)		4.5				
AAC(42)	non	1.5				

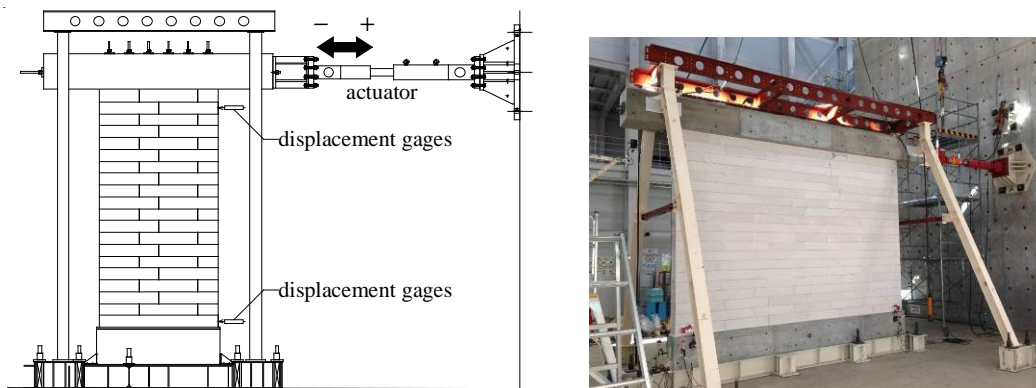


Fig. 4.1 Test setup

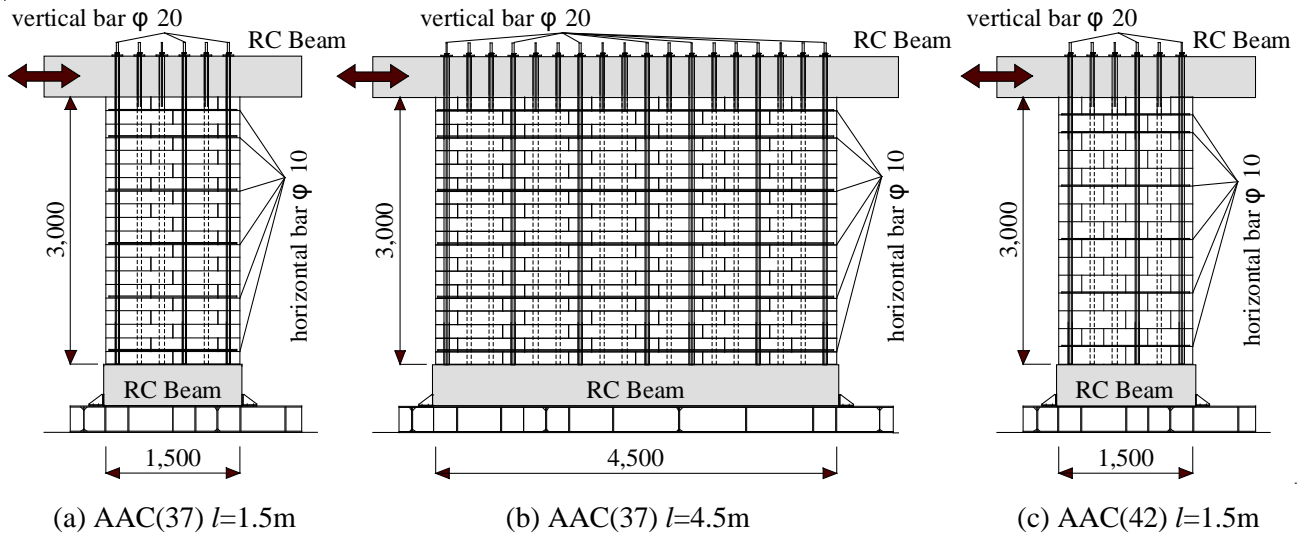


Fig. 4.2 Test specimens

Table 4.2 Target story drift level

<i>l</i> (m)	Target story drift level (rad)
1.5	$\pm 1/2000, \pm 1/1000, \pm 1/500, \pm 1/300, \pm 1/150, \pm 1/100, \pm 1/300, \pm 1/50$ , Monotonic force(+)
4.5	$\pm 1/4000, \pm 1/2000, \pm 1/1500, \pm 1/1000, \pm 1/750, \pm 1/500, \pm 1/250, \pm 1/150$ , Monotonic force(+)

## 4.2 TEST RESULTS AND BEHAVIOR

Test results are shown in Table.4.2. Pictures of the specimens at the end of tests and cracking patterns under positive direction force are shown in Fig. 4.3, force - deformation curves are shown in Fig. 4.4. The force was obtained from the force per wall length.

Integrated behavior was observed in all specimens. It is assumed that each AAC masonry blocks was sufficiently bonded with grout.

The 1.5m wall with AAC(37) developed flexural cracks at 1/941 rad (0.10% drift) and shear cracks at 1/192 rad (0.51% drift). A vertical bar which was applied tension achieved yield strength at 1/186 rad (0.53% drift), then maximum force of 44.7 kN/m was obtained at 1/51 rad (1.96% drift). Force kept 80% of the maximum force in post-peak and the wall failed in shear failure mode at 1/26 rad (3.84% drift).

Table 4.2 Test results:  $P_c, \theta_c, K_c$  (first flexural cracking),  $P_y, \theta_y$  (yield strength),  $P_m, \theta_m$  (maximum force)

specimen	force (kN/m)			deformation (rad)			Stiffness (kN/rad/m)	
	$P_c$	$P_y$	$P_m$	$\theta_c$	$\theta_y$	$\theta_m$	$K_c$	$K_y$
AAC(37) <i>l</i> =1.5m	12.3	36.3	44.7	1/941	1/186	1/51	11574	6752
AAC(37) <i>l</i> =4.5m	29.1	60.2	67.3	1/1454	1/352	1/251	42311	21190
AAC(42) <i>l</i> =1.5m	15.3	35.7	37.7	1/488	1/163	1/34	7466	5819

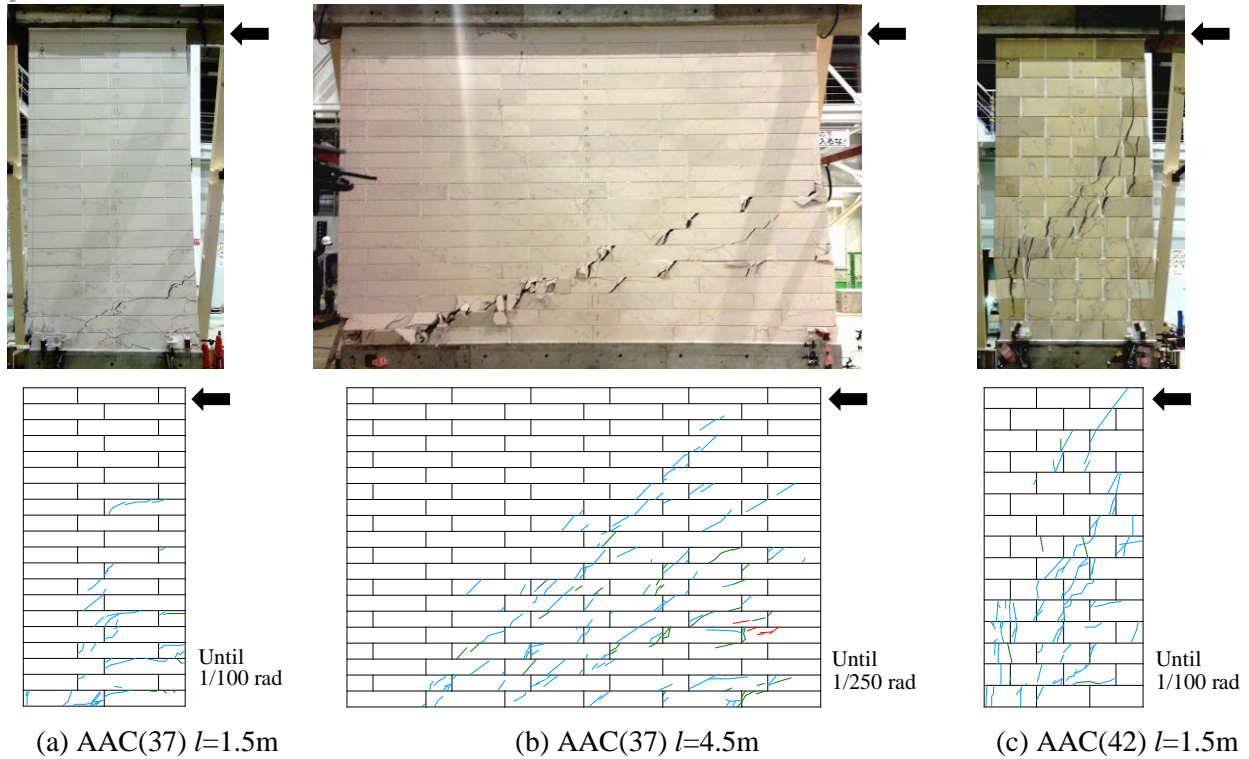


Fig. 4.3 Pictures of the specimens at the end and Cracking patterns under positive direction force

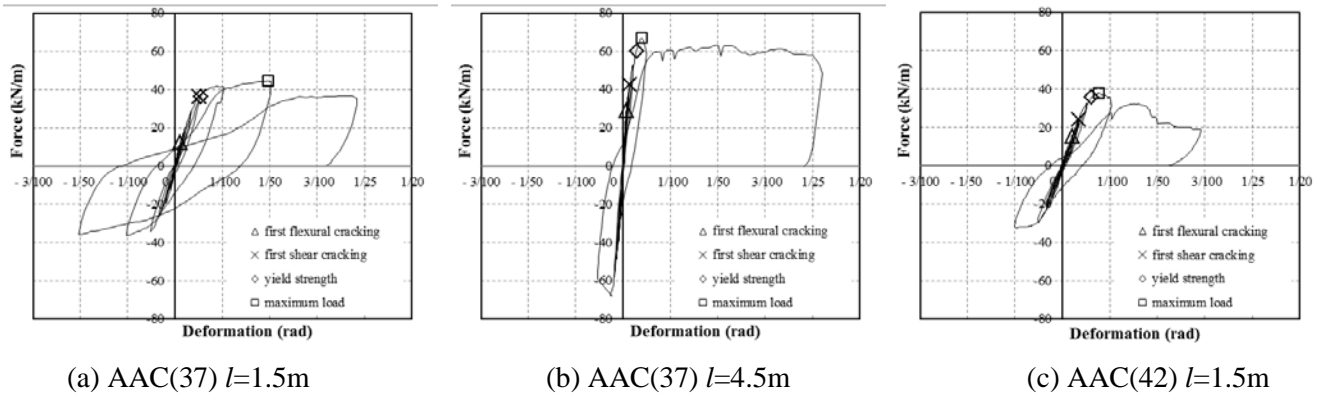


Fig. 4.4 Force - Deformation curves

The 4.5m wall with AAC(37) developed flexural cracks at 1/1454 rad (0.07% drift) and shear cracks at 1/736 rad (0.13% drift). A vertical bar which was applied tension achieved yield strength at 1/352 rad (0.28% drift), then the maximum force of 67.3 kN/m was obtained at 1/251 rad (0.40% drift). Force kept 90% of maximum force in post peak and a horizontal re-bar fractured in shear failure mode at 1/22 rad (4.55% drift). It is noteworthy fact that stiffness per wall length of 4.5m wall was 4 times as large as that of 1.5m wall in the first flexural cracks. It was considered to be due to effect of flexural deformation because flexural ratio (ratio of flexural deformation to sum of the flexural and shear deformation in Fig. 4.5) of 1.5m wall was higher than 4.5m wall. The measure method of the flexural and shear deformation is shown in Fig. 4.6 and the value was given by Eq. 4.1, Eq. 4.2.

The 1.5m wall with AAC(42) developed flexural cracks at 1/488 rad (0.21% drift) and shear cracks at 1/293 rad (0.34% drift). A vertical bar which was applied tension achieved yield strength at 1/163 rad (0.61% drift), then the maximum force of 37.7 kN/m was obtained at 1/131 rad (0.76% drift). Force plunged in post peak and the



wall failed in shear failure mode at 1/34 rad (2.94% drift). It is considered that the internal reinforcements avoid post-peak drop and enhance displacement capacity as with wallette shear tests.

$$x_b = \Sigma ( b_1\delta_i + b_2\delta_i ) ( H - y_i ) / w \quad (4.1)$$

$$x_s = \Sigma L ( s_1\delta_i + s_2\delta_i ) / 2h \quad (4.2)$$

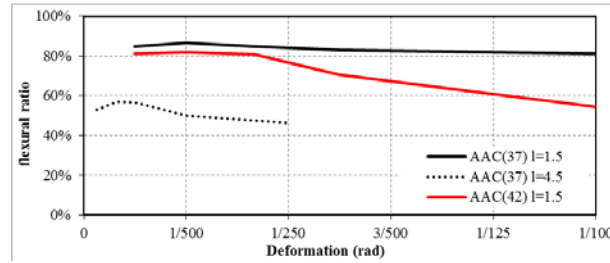


Fig. 4.5 Ratio of flexural deformation to sum of flexural and shear deformation

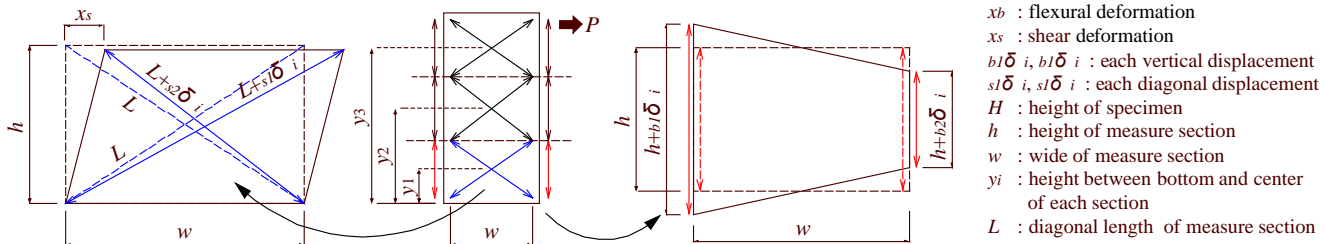


Fig. 4.6 Measure method of flexural and shear deformation

## 5. BASIC CONSIDERATION OF TEST RESULT

### 5.1 HYPOTHESIS AND CALCULATION MODEL

The test results of bearing wall were evaluated by following hypothesis and calculation model. The bearing wall was calculated as a cantilever beam which has an effective cross section,  $A_e$  according to Navier's hypothesis in Fig. 5.1. The AAC and grout were considered as a homogeneous material which has effective compressive strength,  $mF_c$ , Young modulus,  $mE$  and shear modulus,  $mG$  obtained from wallette tests. Tensile strength of the material was provided by tensile strength of AAC,  $aF_t$ . For the sake of easiness, only the vertical reinforcements which were cast in the both ends of the 1.5m long wall were considered. As for the 4.5m long wall, the second reinforcements from both ends also were considered and the sum of two cross sectional area of reinforcements replaced at centroid position. Tensile stress of the material was transferred until  $aF_t$ . Compressive stress of the material was directly proportional to strain of the material until yield moment,  $M_y$ . In ultimate moment of flexural failure mode,  $M_u$ , an equivalent compressive stress block which has the same area as that of actual stress and 85% of effective compressive strength replaced actual compressive stress in Fig. 5.2. The value of  $k_1$  was obtained from compression wallette tests. The vertical reinforcement was considered as elastic perfectly plastic model which has yield point,  $s\sigma_y$  and Young modulus,  $sE$  obtained from the experimental tests.

Each strength,  $P$  was given by Eq. 5.1. Flexural cracking moment,  $M_c$  and deformation,  $\delta_c$  were given by Eq. 5.2 and Eq. 5.3.  $M_y$  was given by Eq. 5.4 and its deformation,  $\delta_y$  was given by Eq. 5.5 assuming that deformation of the beam was directly proportional to its moment.  $M_u$  and its deformation,  $\delta_u$  were given by Eq. 5.6 and Eq. 5.7.  $\delta_u$  was sum of  $\delta_y$  and deformation obtained from rotation of a plastic hinge which height,  $h_d$  was assumed to be

60% of wall length considering behavior of the test results. Shear cracking strength,  $Q_{cr}$  was given by Eq. 5.8 assuming that shear cracking develops when maximum principal stress achieved to  $aF_t$ . Shear deformation,  $\delta_s$  was given by Eq. 5.9 until ultimate strength. Therefore, deformation of shear cracking was not considered.

$$P = M / h \tag{5.1}$$

$$M_c = aF_t Z_e \tag{5.2}$$

$$\delta_c = P_c h^3 / 3_m E I_e \tag{5.3}$$

$$M_y = p_t s \sigma_y \{ (1 - x_{n1})(3 - x_{n1}) - \gamma (x_{n1} - d_{c1})(3d_{c1} - x_{n1}) \} b d^2 / 3(1 - x_{n1}) \tag{5.4}$$

$$\delta_y = s \sigma_y h^2 / 3_s E (d - x_n) \tag{5.5}$$

$$M_u = a_t s \sigma_y (d - k_2 a_t s \sigma_y / k_1 k_3 b_m F_c) \tag{5.6}$$

$$\delta_u = (\varphi_u - \varphi_y) h_d (h - h_d) + \delta_y \tag{5.7}$$

$$Q_{cr} = 2/3 b D a F_t^2 \tag{5.8}$$

$$\delta_s = 6P h / 5_m G b D \tag{5.9}$$

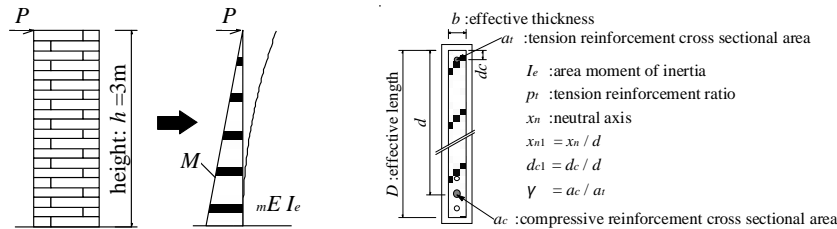


Fig. 5.1 Cantilever beam which has effective cross section

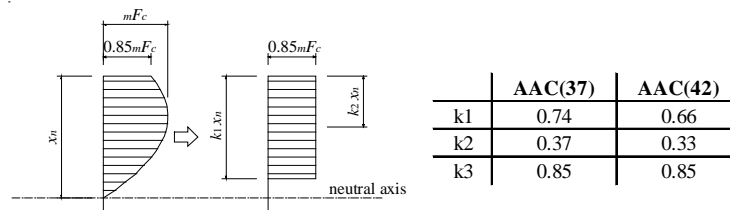


Fig. 5.2 Equivalent stress block in ultimate moment

## 5.2 COMPARISON BETWEEN EXPERIMENTAL RESULTS AND CALCULATION

Comparison between the experimental results and the calculation was shown in Fig. 5.3. Deformation of the calculation was given by sum of the flexural deformation and shear deformation.

As for AAC(37) walls, the flexural cracking strength and deformation obtained from the experimental results were in good agreement with one of calculation, however the shear cracking strength was lower than those calculated value. The stiffness of experimental results after flexural cracking agreed with them of calculation. As for AAC(42) wall, the flexural crackin strength of experimental result showed good agreement with one of



calculation, however the flexural cracking deformation and shear crackin strength did not. It is supposed that vertical crackings observed on surfaces of the wall in the initial stage of the test; they were not observed in the wallette tests, was not considered. The yield strength and ultimate strength of AAC(37) and AAC(42) walls obtained from experimental results were higher than that of calculation. It is supposed that the vertical reinforcements which were cast in only both ends of the walls were considered. The deformation of peak force was approximately agree with that of calculation.

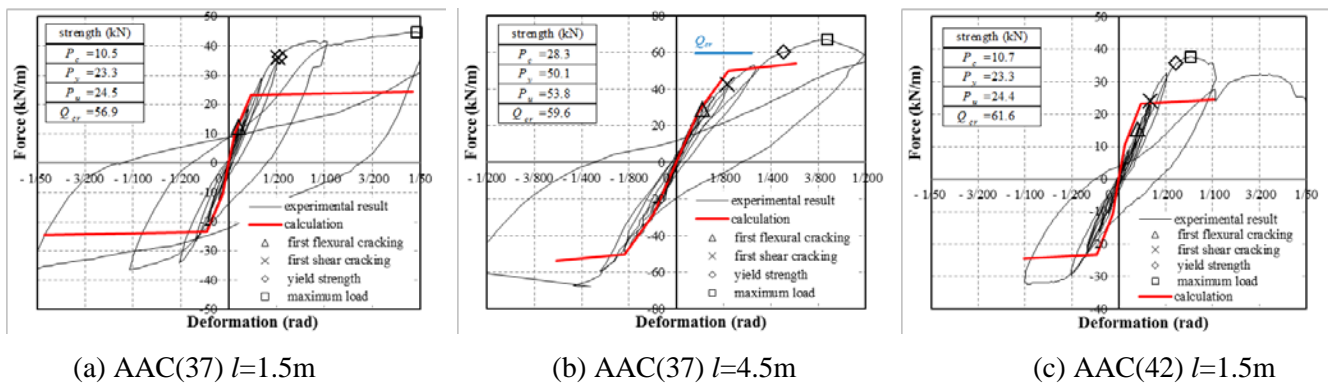


Fig. 5.3 Comparison between experimental results and calculation

## 6. CONCLUSIONS

In-plane behavior of bearing walls composed of different types of blocks were observed. Two of them was used with reinforced blocks, the other was used with unreinforced blocks. Then they were compared with each other based on the difference in the wall length and the type of blocks. From the test results, the integration behavior was confirmed in the bearing wall. That resulted from the AAC blocks which were sufficiently bonded each other with grout. The internal reinforcement avoided sharp post-peak loss of strength and enhanced its displacement capacity. Moreover the stiffness per wall length of the 4.5m wall was higher than that of the 1.5m wall which suggests that the flexural deformation of the 4.5m wall was lower than that of the 1.5m wall.

In addition, this paper provided basic consideration of the bearing wall test results referring to ordinary RC beams. The mechanical properties of the materials and masonry wall were clarified from the material tests and wallette tests. From the comparison between the exerimental results and the calculation, the flexural cracking strength in the experiments was found in good agreement with that in the calculation, however the shear cracking strength in the experiments lower than that calulated values. The flexural cracking deformation of the wall built with reinforced blocks in the test results agreed well with that calculation. The yield and ultimate strengths obtained from experiments were higher than those calculated values respectively because the vertical reinforcements at only the both ends of the walls were incorporlated in the calclation procedure. The fact repsents the need for the calculation model to be modified for better calculation precision.

## ACKNOWLEDGEMENTS

The authors would like to thank the Yokohama National University's students (at the time) and a technical officer who supported the experimental tests.

## REFERENCES

- [1] Penna A, Magenes G, Calvi GM, Costa AA (2008): Seismic performance of AAC infill and bearing walls with different reinforcement solutions. *14<sup>th</sup> International brick and block masonry conference*, Sydney, Australia.
- [2] Japan Association for Building Research Promotion (2004): *Guidelines for Structural Design of Reinforced Masonry (RM) Structures*. (in Japanese)